Supporting Information

Surface plasmon enhanced drug efficacy using core shell Au@SiO_2 nanoparticle carrier

Zhiqin Chu[a], Chun Yin[b], Silu Zhang[a], Ge Lin[b,*], Quan Li[a,*]

[a]Department of Physics, The Chinese University of Hong Kong, Shatin, New Territories, Hong Kong

[b]School of Biomedical Sciences, Faculty of medicine, The Chinese University of Hong Kong, Shatin, New Territories, Hong Kong

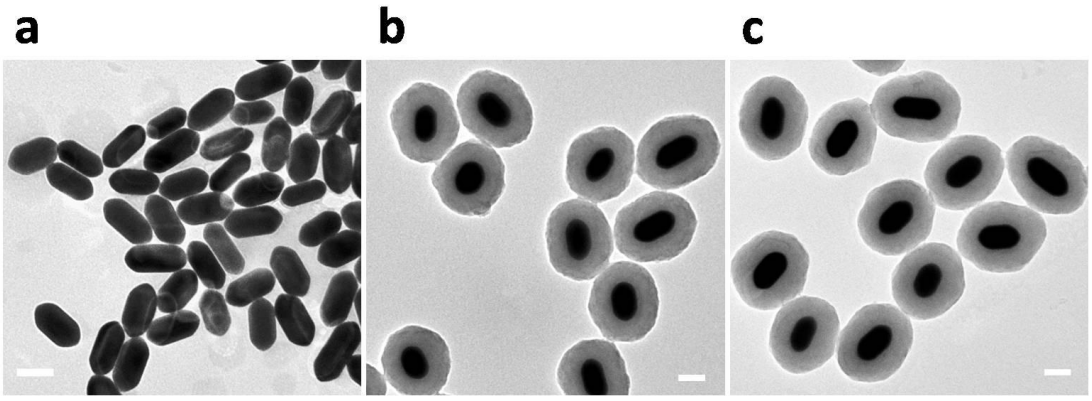

Fig. S1 TEM images depicting the synthesis process of Au@(SiO_2-MB) NPs. Low magnification TEM images of (a) Au NRs, (b) Au@SiO_2 NPs and (c) Au@(SiO_2-MB) NPs. (All scale bars are 50 nm.)

One should notice that, the Au@SiO_2NP had similar size as the Au@(SiO_2-MB) NP. This result suggested that encapsulating MB into the silica shell does not affect the morphology of the core-shell NPs.

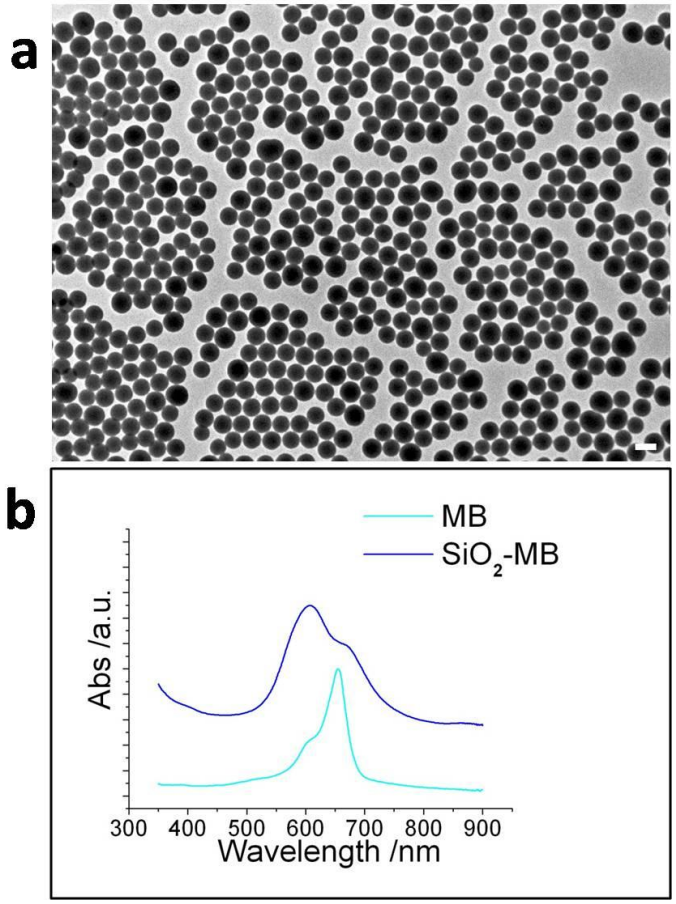

Fig. S2 Characterization of SiO_2-MB NPs. (a) TEM image of the SiO_2-MB NPs. (b)UV/Vis absorption spectra of the MB alone and SiO_2-MB NPs in aqueous solution. The scale bar is 200 nm.

The average diameter of SiO_2-MB is ~150 nm (FigureS2a), and its UV/Vis absorption spectra is shown in Figure S2b, in which the characteristic absorption peaks of MB could be easily observed (~600 nm and ~660 nm).

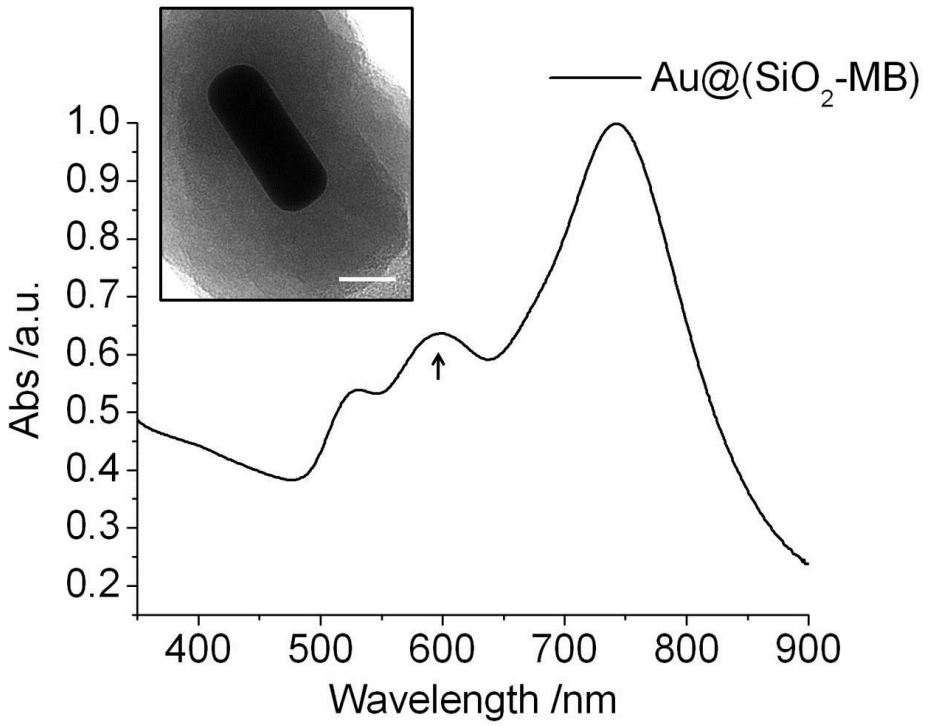

Fig. S3 Characterization of Au@(SiO_2-MB) NPs. Normalized UV/Vis absorption spectrum of the Au@(SiO_2-MB)NPs in aqueous solution (Original longitudinal plasmon wavelength of Au NR is ~700 nm), insert is low magnification TEM image of one selected Au@(SiO_2-MB) NP. The scale bar is 20 nm; Arrow head points to the characteristic peak of MB dimer.

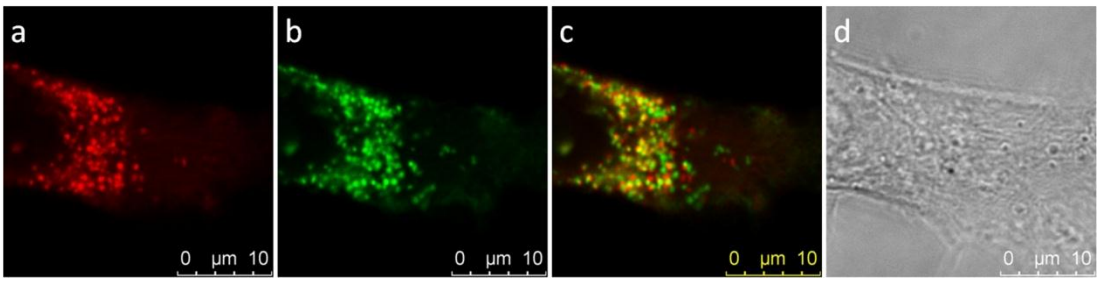

Fig. S4 Confocal microscopy images showing the localization of Au@(SiO_2-MB) NPs in HepG2 cells (live cell): (a) the red fluorescence of NPs (signal of MB) indicates the localization of NPs inside cells; (b) the green fluorescence of Lysotracker Green indicates the localization of lysosomes in cells; (c) overlapping image of a and b, the yellow signal originates from the overlapping red and green florescence signals, indicating that most of the NPs are located in the lysosomes; (d) transmittance images showing the morphology of HepG2 cells.

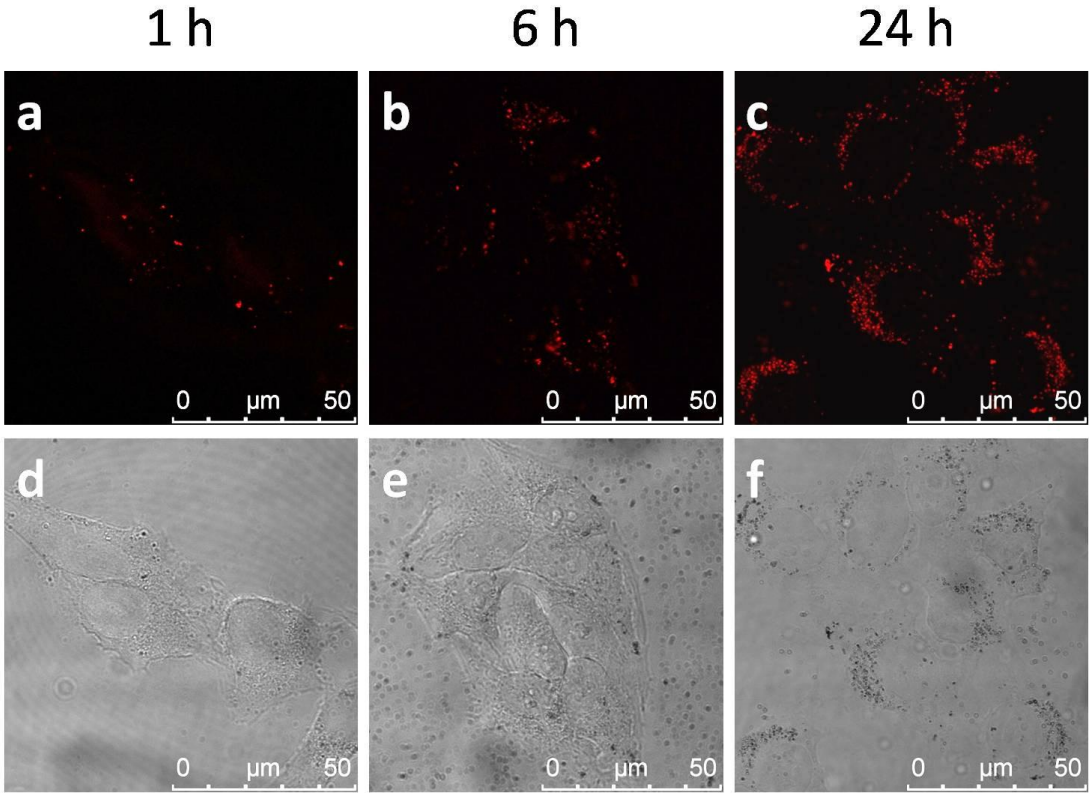

Fig. S5 Time dependent cellular uptake of Au@(SiO_2-MB) NPs. Confocal microscopy images of HepG2 cells incubated with Au@(SiO_2-MB) NPs for different incubation periods. Fluorescent images (red, MB signal) of cells incubated with Au@(SiO_2-MB) NPs for (a)1 hour, (b)6 hours and (c) 24 hours; transmittance images of cells incubated with Au@(SiO_2-MB) NPs for (d)1 hour, (e)6 hours and (f) 24 hours.

Table S1 Leaching test of MB-loaded NPs in DMEM medium. The MB-loaded NPs were dispersed in DMEM medium for 1, 6 and 24 hours at 37^{o}C, and then the NPs were centrifuged down. The leakage of MB was calculated from its UV/Vis absorption in the supernatant.

Time / hour	**1**	**6**	**24**
Au@(SiO_2-MB)	**NA**	**NA**	**13%**

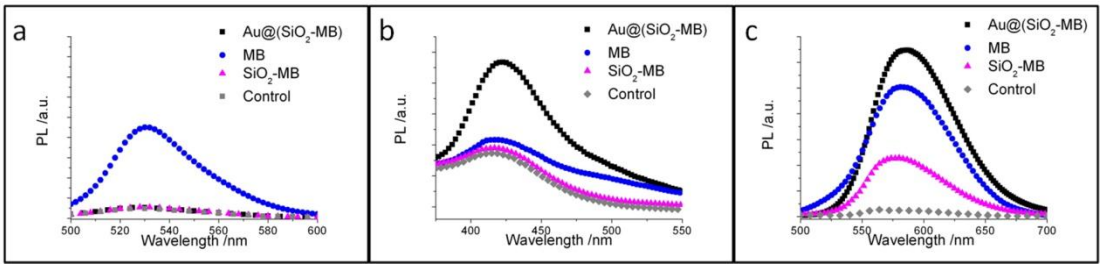

Fig. S6 Fluorescence spectra of free MB, SiO_2-MB NPs and Au@(SiO_2-MB)NPs after 20 minutes irradiation with 590 nm LED (a)in 5×10^{-5} M aqueous singlet oxygen sensor green (SOSG) solution with Ex: 488 nm; (b) in 5×10^{-4} M NaOH (2×10^{-3}) solution of terephthalic acid (TA)with Ex: 315 nm; and (c) in 5×10^{-5} M aqueous dihydroethidium (DHE) with Ex: 470 nm. In all experiments de-ionized water containing the detection dye was chosen as the control. The concentration of MB was fixed as 5 μM in all samples.

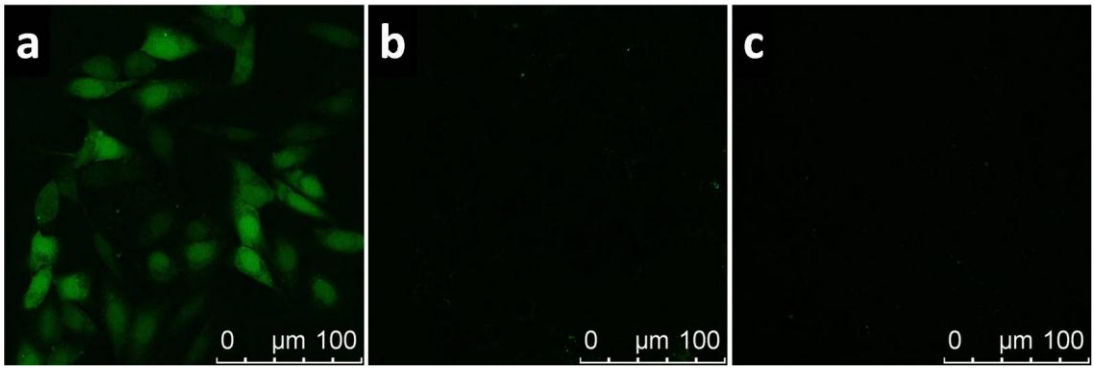

Fig. S7 Detection of intracellular ROS level of HepG2 cells by confocal microscopy. Confocal images depicting the intracellular ROS level of HepG2 cells treated with (a) Au@(SiO_2-MB) NPs, (b) Au@SiO_2 NPs and (c) serum free medium (control) for 24 hours then irradiated with 590 nm LED for 20 minutes. The ROS signal was measured by carboxy-H_2DFFDA and proportional to the intensity of the green fluorescence (carboxy-H_2DFFDA).

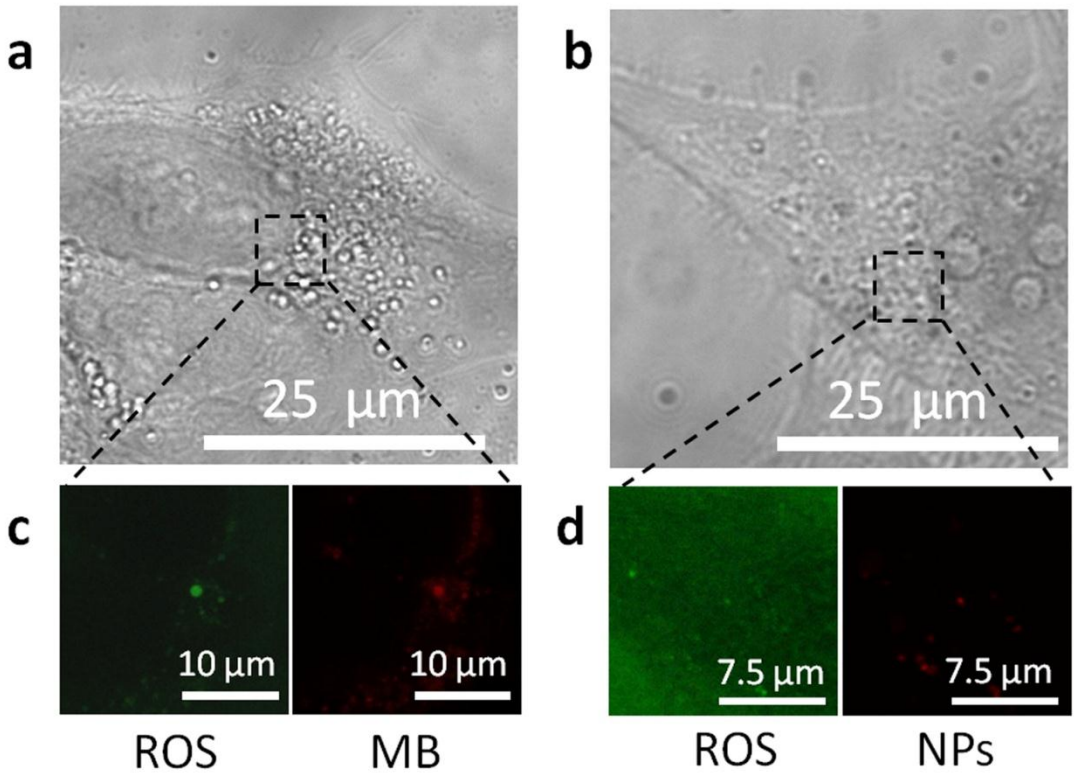

Fig. S8 Comparison of ROS generation in a typical HepG2 cell incubated with free MB or Au@(SiO2-MB) NPs for 24 hours ([MB] =0.5 µM). **a,b,**Transmittance images showing part of the HepG2 cells. The boxed region was chosen for real-time monitoring of ROS generation; **c,d,** The ROS level recorded from the corresponding regions of (a) and (b) at the end of 8 minutes' irradiation. The ROS signal was measured by carboxy-H_2DFFDA (green color). The physical location of NPs was determined using the MB fluorescence signal (red color).

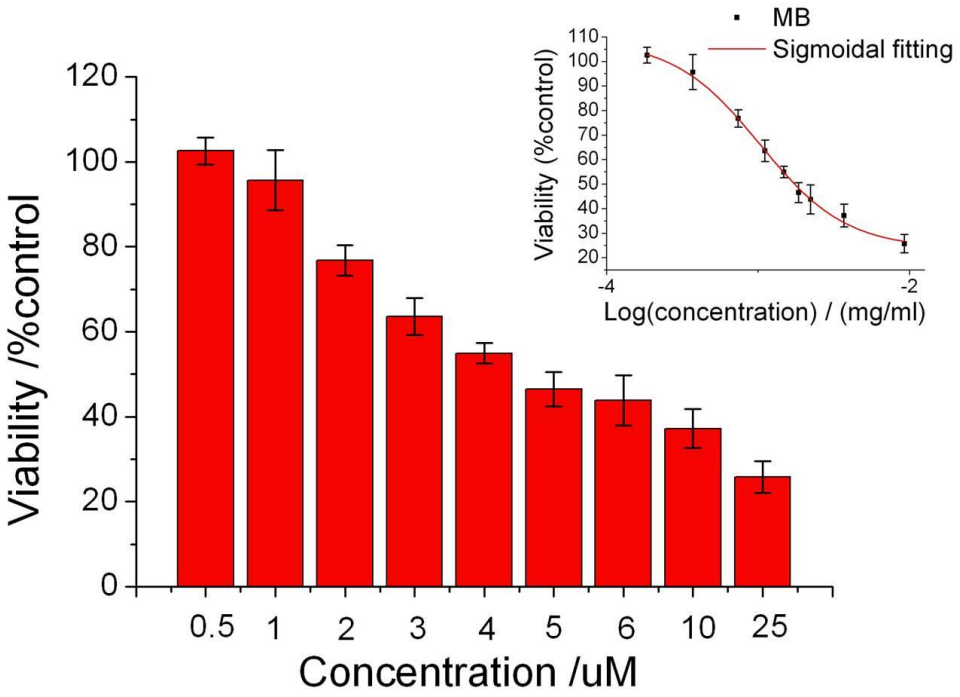

Fig. S9 Viability (by MTT assay) of the HepG2 cells incubated with MB for 24 hours, insert is the sigmoidal fitting of the obtained viability curve. All data were shown as mean ± SD (from three independent experiments) and significantly different ($p < 0.05$) from control (analyzed by Student's t test).The R^2 of sigmoidal fitting was 0.98.

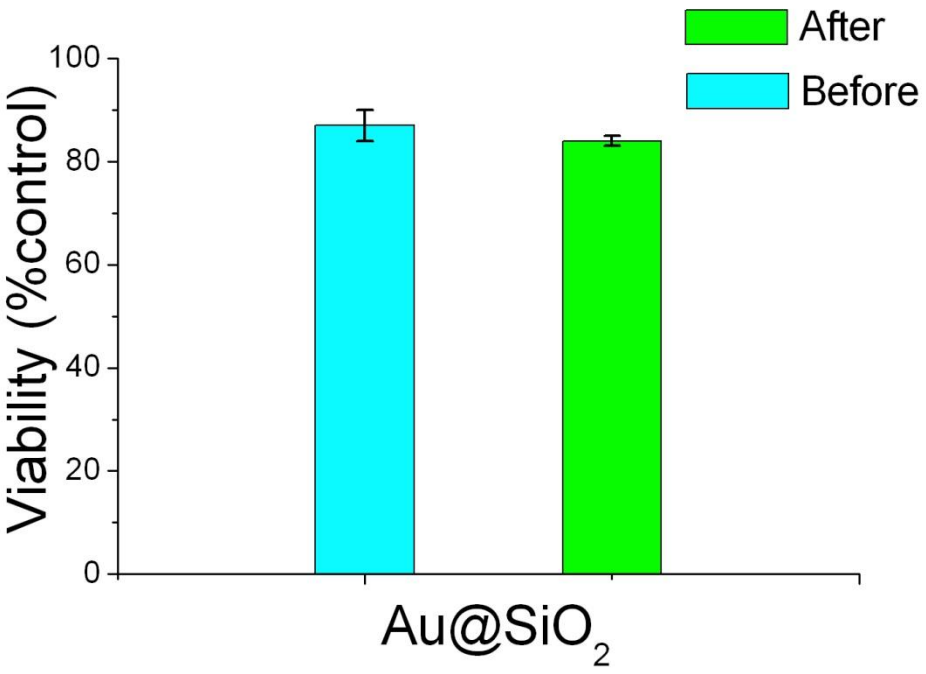

Fig. S10 Effect of light irradiation on the HepG2 cells incubated with $Au@SiO_2$ NPs (without MB).Viability (by MTT assay) of the HepG2 cells treated with $Au@SiO_2$ NPs before and after LED irradiation for 20 minutes. All data were shown as mean $\pm$ SD(from three independent experiments) and significantly different ($p < 0.05$) from control (analyzed by Student's t test).

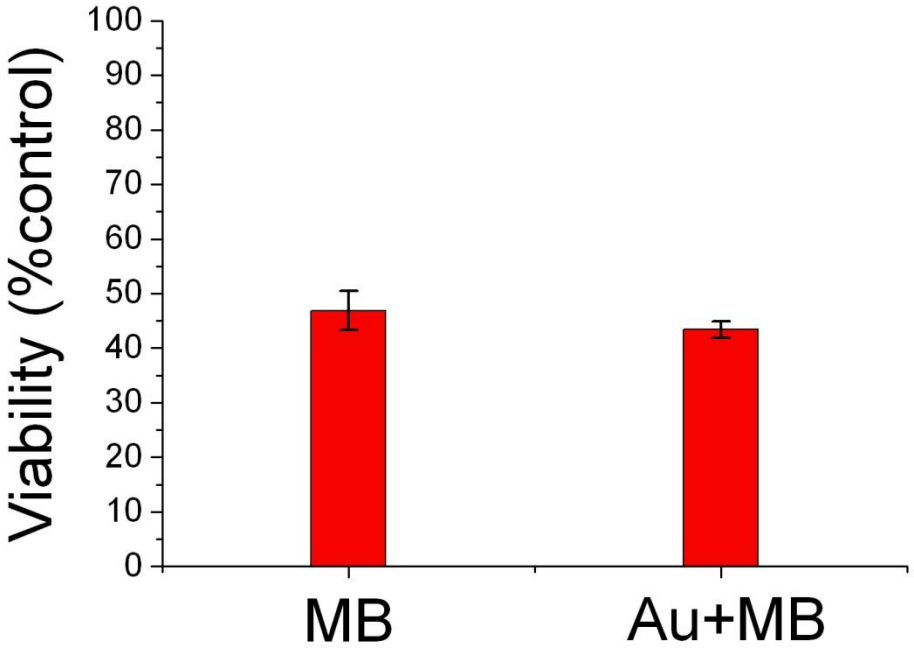

Fig. S11 Comparison of the HepG2 cells' viability (by MTT assay), when they are incubated with MB or MB mixed with Au NRs (Au+MB) for 24 hours. The corresponding longitudinal mode of Au SPR wavelength is 600 nm. The concentration of MB is 5 μM for both of the samples. All data were shown as mean ± SD (from three independent experiments) and significantly different ($p < 0.05$) from control (analyzed by Student's t test).

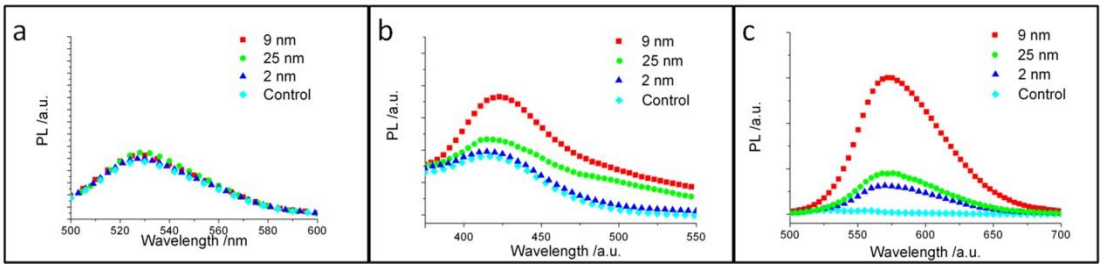

Fig. S12 Fluorescence spectra of Au@(SiO_2-MB)NPs with different spacer SiO_2layer thickness (~2 nm, ~9 nm, and ~25 nm, respectively) after 20 minutes irradiation with 590 nm LED in (a)5×10^{-5} M aqueous singlet oxygen sensor green (SOSG) solution with Ex: 488 nm; (b) 5×10^{-4} M NaOH (2×10^{-3}) solution of terephthalic acid (TA)with Ex: 315 nm; and (c) 5×10^{-5} M aqueous dihydroethidium (DHE) with Ex: 470 nm. In all experiments de-ionized water containing the corresponding detection dyes were chosen as the control. The concentration of MB was fixed as 5 μM in all samples.

Literature work suggested that the plasmonic effect would decay as a function of the separation distance between the nobel metal nanostructure and the active optical agent (MB in the present case). On the other hand, direct contact between the two would cause quenching effect. We therefore conducted this experiment, trying to find out the optimum spacer SiO_2 layer thickness for the NPs. We found that uniform and completely wrapping the Au NR was difficult at small SiO_2 layer thickness (e.g. 2nm) , and thus cannot avoid quenching effect. On the other hand, very large spacer layer thickness (e.g. 25 nm) only led to weak plamonic effect. Therefore, the thickness of spacer SiO_2 layer was chosen as 9 nm in the present work. One can see

from Figure S1 that such Au@(SiO_2-MB) NPs lead to the most ROS (both hydroxyl oxide and superoxide) generation among the three.

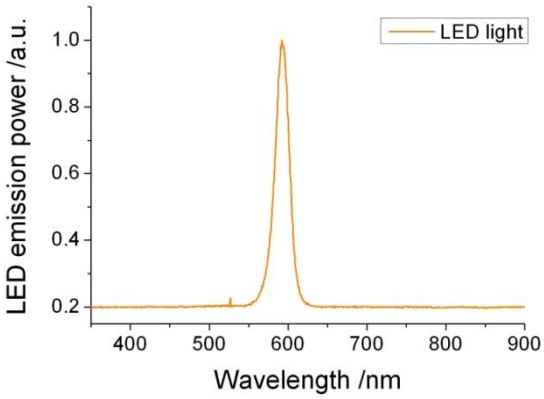

Fig. S13 LED emission profile of the 590 nm LED used in the present study.

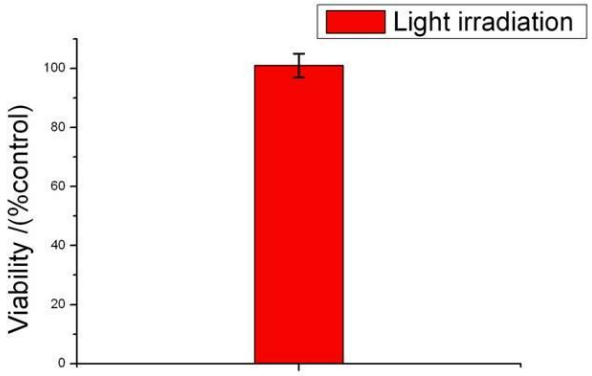

Fig. S14 Viability of HepG2 cells after irradiation with 590 nm LED light for 20 minutes. All data were shown as mean ± SD(from three independent experiments) and significantly different ($p < 0.05$) from control (analyzed by Student's t test).

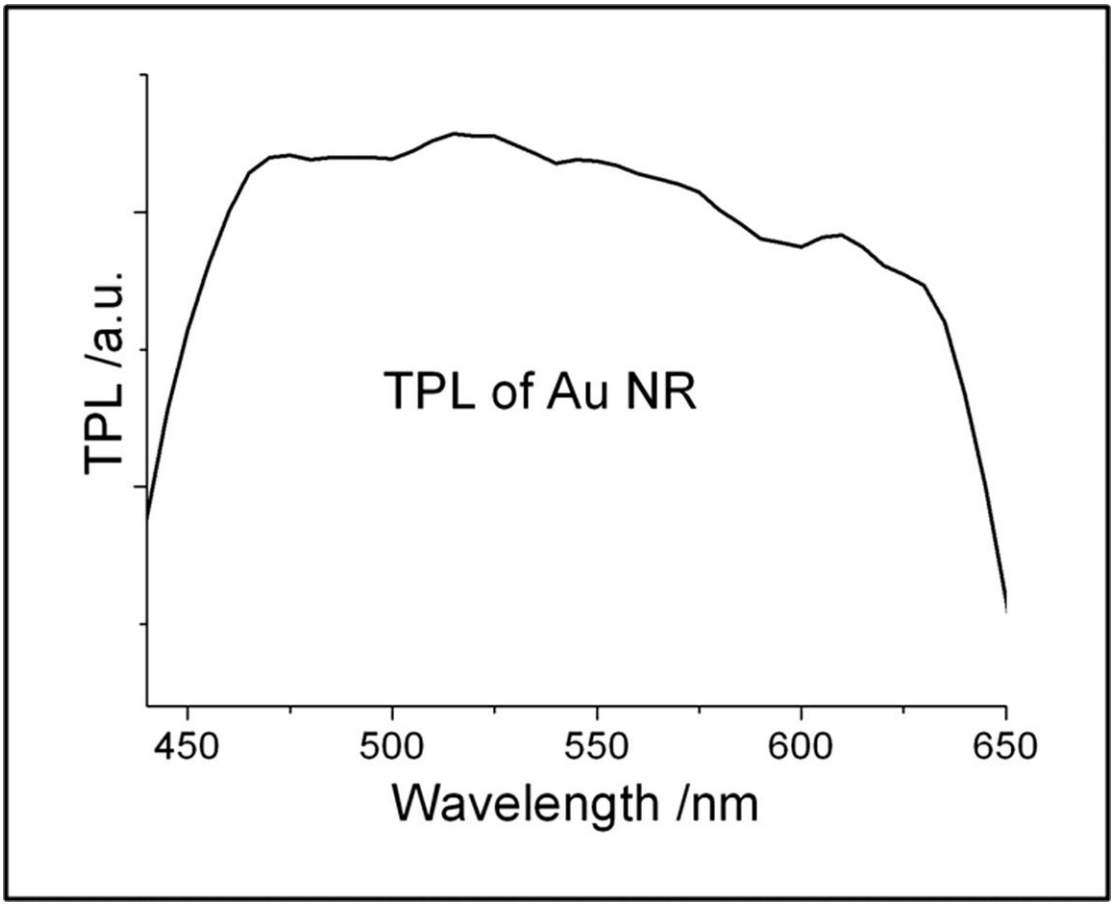

Fig. S15 Two photon luminescence spectrum of Au NRs.